



ELSEVIER

8 October 2001

Physics Letters A 289 (2001) 59–65

PHYSICS LETTERS A

www.elsevier.com/locate/pla

# Erupting, flat-top, and composite spiral solitons in the two-dimensional Ginzburg–Landau equation

L.-C. Crasovan<sup>a,b</sup>, B.A. Malomed<sup>c</sup>, D. Mihalache<sup>a,b,\*</sup>

<sup>a</sup> Department of Theoretical Physics, Institute of Atomic Physics, PO Box MG-6, Bucharest, Romania

<sup>b</sup> Research Center in Optical Engineering and Photonics, Bucharest Polytechnical University, 77206 Bucharest, Romania

<sup>c</sup> Department of Interdisciplinary Sciences, Faculty of Engineering, Tel Aviv University, Tel Aviv 69978, Israel

Received 19 February 2001; received in revised form 11 July 2001; accepted 28 August 2001

Communicated by A.R. Bishop

## Abstract

We present three novel varieties of spiraling and nonspiraling axisymmetric solitons in the complex cubic–quintic Ginzburg–Landau equation. These are irregularly “erupting” pulses and two different types of very broad stationary ones found near a border between ordinary pulses and expanding fronts. The region of existence of each pulse is identified numerically. We test their stability and compare their features with those of their counterparts in the one-dimensional and conservative two-dimensional models. © 2001 Elsevier Science B.V. All rights reserved.

PACS: 42.65.Tg; 47.32.Cc

Keywords: Localized pulse; Complex Ginzburg–Landau equation; Spiral soliton

## 1. Introduction

Ginzburg–Landau (GL) equations provide for a universal description of pattern formation in various types of nonlinear dissipative systems, see Refs. [1–28] and references therein. Equations of this type also describe generation of soliton-like light pulses in mode-locked fiber lasers with fast saturable absorbers [20,22]. These mode-locked soliton fiber lasers are of much interest to various applications because they can generate pulse arrays with a wide range of durations and repetition rates.

Patterns described by GL equations in two dimensions are of special interest. In particular, steady “spiral solitons”, i.e., localized (“bright”) two-dimensional

(2D) objects with *internal vorticity*, which are characterized by an integer-valued “spin”  $S$ , were studied in a recent work [24] within the framework of the complex cubic–quintic (CQ) GL equation. In that work, it has been shown that spiral solitons, stable against all modes of small perturbations, including azimuthal ones which are fatal for the vortex rings governed by the conservative nonlinear Schrödinger (NLS) equation [29], can be readily found in the CQ GL equation. The aim of the present work is to demonstrate that the same general model gives rise to other novel types of nonstationary and stationary axisymmetric solitons, with and without the intrinsic vorticity.

We consider the  $(2 + 1)$ -dimensional complex GL equation in a generic form,

$$iA_z + i\delta A + (1/2 - i\beta)(A_{xx} + A_{yy}) + (1 - i\varepsilon)|A|^2 A - (v - i\mu)|A|^4 A = 0, \quad (1)$$

\* Corresponding author.

E-mail address: mihalake@theory.nipne.ro (D. Mihalache).

where the subscript stands for the partial derivative. The equation is written in the “optical” notation, assuming evolution along the propagation coordinate  $z$  of a light beam with its 2D cross section in the plane  $(x, y)$ . In fact, bulk (three-dimensional) optical media is the most appropriate system for the experimental generation of bright vortex solitons (vortex rings), even if they are unstable [30]. In this case,  $A(z, x, y)$  is the local amplitude of the electromagnetic wave, the diffraction and cubic self-focusing coefficients are normalized to be 1,  $\varepsilon$  is the nonlinear gain,  $\delta$  and  $\mu$  are the linear and quintic loss parameters (the latter one actually accounts for the nonlinear gain saturation in optical media), and  $\nu$  is the quintic self-defocusing coefficient. Lastly,  $\beta$  is an effective diffusion coefficient. It is not a standard part of the propagation equation for optical media, but it appears if light creates free charge carriers, which may take place in semiconductor waveguides. Due to their physical meaning, all these coefficients are positive.

The spiral solitons are axisymmetric solutions to Eq. (1) of the form  $A(z, x, y) = U(z, r) \exp(iS\theta)$ , where  $r$  and  $\theta$  are polar coordinates in the  $(x, y)$  plane, and  $S$  is the integer “spin” (topological charge of the vortex). The complex amplitude  $U(z, r)$  obeys an equation obtained after the substitution of the latter expression into Eq. (1),

$$iU_z + i\delta U + (1/2 - i\beta)(U_{rr} + r^{-1}U_r - S^2r^{-2}U) + (1 - i\varepsilon)|U|^2U - (\nu - i\mu)|U|^4U = 0. \quad (2)$$

Spiral-soliton solutions to Eq. (2) are singled out by boundary conditions stating that  $U \sim r^S$  as  $r \rightarrow 0$ , and  $U(r)$  decays exponentially as  $r \rightarrow \infty$ . Note that the localized solution with  $S \neq 0$  may be interpreted as a *spiraling* soliton because the function  $U(r)$  is complex,

$$U(z, r) \equiv |U(z, r)| \exp(i\Phi(z, r)), \quad (3)$$

hence constant-phase curves  $S\theta + \Phi(r) = \text{const}$ , taken at a fixed value of the propagation distance  $z$ , are spirals, rather than straight lines  $S\theta = \text{const}$ , as in the case of the CQ NLS equation, where  $U(r)$  is real [29, 31, 32].

In this work, our first purpose is to search for irregularly pulsating but robust (nondecaying) axisymmetric (both spiraling,  $S = 1$ , and nonspiraling,  $S = 0$ ) soliton solutions to Eq. (2) of the *erupting* type, similar to

those recently found in the one-dimensional (1D) CQ GL equation [19, 20]. Generally, they may be regarded as patterns belonging to a class of pulses with chaotic intrinsic dynamics, which are known in 1D nonlinear systems of the reaction–diffusion type [21].

Additionally, we present two new types of stationary broad axisymmetric localized patterns found in the framework of the same model, which we term *composite* and *flat-top* 2D solitons, similar to their 1D counterparts discussed in detail in Refs. [16–18]. These are very broad pulses residing near a border which separates stationary pulses proper and nonstationary expanding axisymmetric domains.

As the underlying equation (1) contains five independent parameters, an exhaustive analysis of the model in its full parametric space is virtually impossible. Therefore, throughout the Letter we consider two different sets of parameters, characterized by fixed values of three parameters: (i)  $\delta = 0.05$ ,  $\beta = 0.03$  and  $\mu = 0.2$ ; and (ii)  $\delta = 0.1$ ,  $\beta = 0.08$  and  $\mu = 0.1$ . The remaining two parameters  $\nu$  and  $\varepsilon$  will be varied, in order to study transitions between solutions of different types. According to our simulations, these cases are quite representative to display new types of the 2D solitons.

## 2. Erupting solitons

The first finding of our analysis is that direct simulations of the radial equation (2) indeed produce robust “erupting” axisymmetric solitons, and their existence domain is quite large, similar to the 1D case reported in Refs. [19, 20]. A quasi-period of the evolution of a typical erupting spiraling pulse, with the spin  $S = 1$ , is displayed in Fig. 1.

Similar to what has recently been found in the 1D case [19, 20], the eruptions happen irregularly (i.e., chaotically, in the sense of the dynamical chaos), although each quasi-period contains one eruption. To demonstrate the irregularity of the spiral-soliton’s intrinsic dynamics, in Fig. 2 we display a generic dynamical trajectory in the plane of the soliton’s average width in the  $x$ -direction,  $\sigma_x \equiv \sqrt{\langle x^2 \rangle - \langle x \rangle^2}$ , and the soliton’s mean width in the  $k_x$ -direction of the Fourier space,  $\sigma_{k_x} = \sqrt{\langle k_x^2 \rangle - \langle k_x \rangle^2}$ , where  $k_x$  is the  $x$ -component of the wavenumber. The spatial average

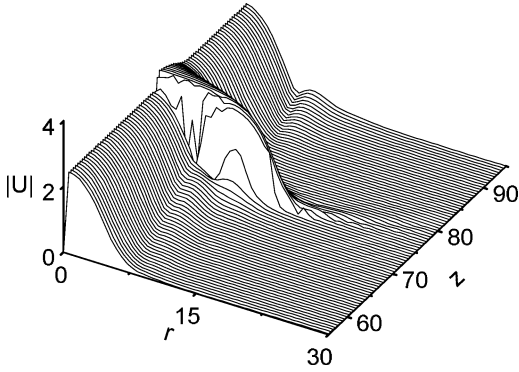


Fig. 1. A quasi-period of the evolution of a spiraling soliton with the spin  $S = 1$ , including one “eruption”. The parameters are:  $\beta = 0.05$ ,  $\delta = 0.05$ ,  $\nu = 1.4$ ,  $\mu = 0.2$  and  $\varepsilon = 1.75$ .

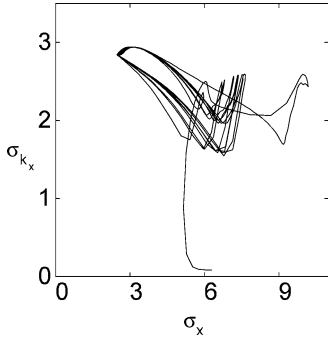


Fig. 2. A trajectory, in the plane  $(\sigma_x, \sigma_{k_x})$ , of the erupting soliton from Fig. 1 illustrating its chaotic intrinsic dynamics.

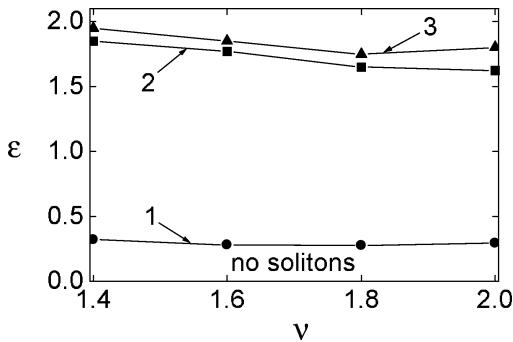


Fig. 3. Existence domains of the two-dimensional erupting solitons. The fixed parameters are:  $\beta = 0.05$ ,  $\delta = 0.05$  and  $\mu = 0.2$ . Circles: a boundary between erupting solitons and the region where the solitons do not form; squares: a boundary between erupting and ordinary (stationary) spiraling solitons; triangles: a boundary between erupting and ordinary nonspiraling (zero-spin) solitons.

of the function  $g(x, y)$  is

$$\langle g(x, y) \rangle \equiv I^{-1} \iint dx dy |U(x, y)|^2 g(x, y),$$

whereas the average of the function  $h(k_x, k_y)$  is given by

$$\langle h(k_x, k_y) \rangle \equiv I^{-1} \iint dk_x dk_y |\tilde{U}(k_x, k_y)|^2 h(k_x, k_y),$$

where  $\tilde{U}(k_x, k_y)$  is the Fourier transform of  $U(x, y)$ . Here

$$I \equiv \iint dx dy |U(x, y)|^2 = 2\pi \int_0^\infty |U(r)|^2 r dr \quad (4)$$

is the soliton’s intensity.

The evolution trajectory presented in Fig. 2 pertains to the soliton shown in Fig. 1 and comprises the first 200 units of the propagation length, which includes several successive eruptions. Notice that, due to the axial symmetry of the erupting solution, one has  $\sigma_y = \sigma_x$  and  $\sigma_{k_y} = \sigma_{k_x}$ . One can see that the trajectory never repeats itself, although in each quasi-period it passes through the same point, corresponding to the soliton at the nonerupting stage of the evolution. This result is similar to that obtained for the erupting 1D nonspinning solitons of the CQ GL equation [20]. We stress that no solution with a strictly periodic sequence of eruptions has been found.

The spiraling erupting solitons are unstable against azimuthal perturbations. As an example, the numerical study of the full equation (1), linearized around the solution with  $S = 1$  (the same as is shown in Fig. 1) at its stationary (nonerupting) stage, yields the result that a perturbation with the azimuthal index  $n = 2$ , which corresponds to a perturbation eigenmode  $\delta A \sim \exp(2i\theta + \sigma z)$ , has the eigenvalue  $\sigma = 0.95 + i60.6$ .

A region in the parameter plane  $(\nu, \varepsilon)$  where erupting solitons have been found in the simulations of Eq. (2) is shown in Fig. 3 for a representative set of parameters. No solitons exist below the curve 1 in Fig. 3. The spiraling (spinning) erupting solitons coexist with the nonspiraling (zero-spin,  $S = 0$ ) erupting ones in the region between the curves 1 and 2, whereas in the small region between the curves 2 and 3 erupting solitons only with  $S = 0$  have been found. The curves 2 and 3 represent borders between erupting and ordinary (stationary) pulses with  $S = 1$  (spiraling)

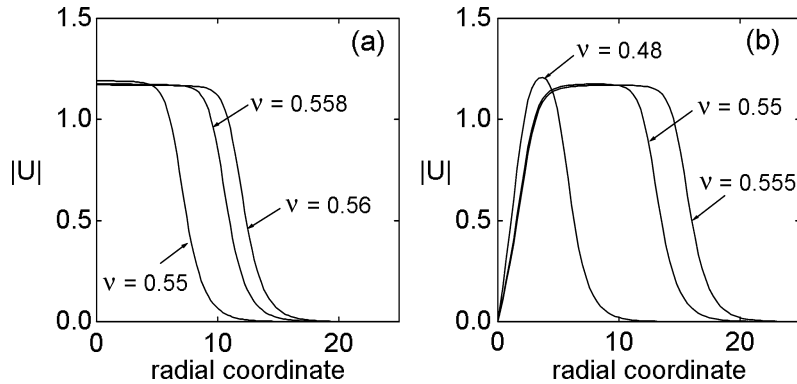


Fig. 4. Radial profiles of (a) nonspirling,  $S = 0$ , and (b) spiraling,  $S = 1$ , flat-top solitons at slightly different values of the quintic self-focusing parameter  $\nu$ , while the other parameters are fixed:  $\beta = 0.03$ ,  $\delta = 0.05$ ,  $\mu = 0.2$  and  $\varepsilon = 0.3$ . Note that the spiraling soliton pertaining to  $\nu = 0.48$  in panel (b) is still an ordinary stationary soliton, rather than a flat-top one.

and  $S = 0$  (nonspirling), respectively. Thus, erupting and ordinary solitons with the same value of the spin do not coexist; however, in the above-mentioned narrow stripe between the curves 2 and 3, the erupting zero-spin solitons coexist with the ordinary ones having  $S = 1$ .

Note that, for the parameter range displayed in Fig. 3, the boundaries between the regions where ordinary solitons and erupting pulses exist, only slightly depend on the quintic self-defocusing coefficient  $\nu$ . We have also observed that, quite naturally, the coefficient  $\mu$ , which accounts for the quintic losses and is thus responsible for the global stability of the model, affects the structure of the model's phase diagrams much stronger.

Lastly, it is relevant to stress that, in contrast with recently studied 1D GL models, both CQ [19,20] and two-component cubic [15] ones, our calculations show that, at all the parameter values considered, *no* regular (strictly periodic) oscillating pulses exist in the 2D GL model.

### 3. Flat-top and composite solitons

Other new dynamical features were found in the present model near a border in the parametric space between the ordinary stationary pulses and *front* solutions (i.e., those describing an indefinitely expanding axisymmetric domain; along with the stationary

pulses, they were found in Ref. [24]). Accurate search in a vicinity of the border has revealed the existence of a transient layer, instead of the sharp frontier, which is filled by two new species of stationary spiraling and nonspirling pulses, to be called *flat-top* and *composite* ones. Both species differ from the ordinary stationary pulses, which were studied in detail in Ref. [24], in that they are very broad. This is quite natural, as the flat-top and composite pulses provide for a crossover from ordinary, relatively narrow, ones to indefinitely expanding fronts. Typical examples of the radial profiles of the flat-top and composite solitons, with  $S = 0$  and  $S = 1$ , are displayed in Figs. 4 and 5. One may see that a very small change of the quintic self-defocusing coefficient  $\nu$  drastically affects the soliton's radial size (note a difference with the situation in Fig. 3 which showed no sensitivity to the value of  $\nu$ ; an explanation for the difference is that the solitons of the flat-top and composite types exist in a very narrow stripe of the phase space). Three-dimensional images of the spiraling solitons of both flat-top and composite types are shown in Fig. 6.

A distinction between the flat-top and composite solitons is that the interior of the former one is a really very flat, while the latter one has an inflexion point, and it is, effectively, composed of different radial layers (hence its name). Although the difference may seem tiny, it leads to dramatic differences in dynamical properties of these two species of the pulses: the flat-top spiral solitons are completely stable (see below),

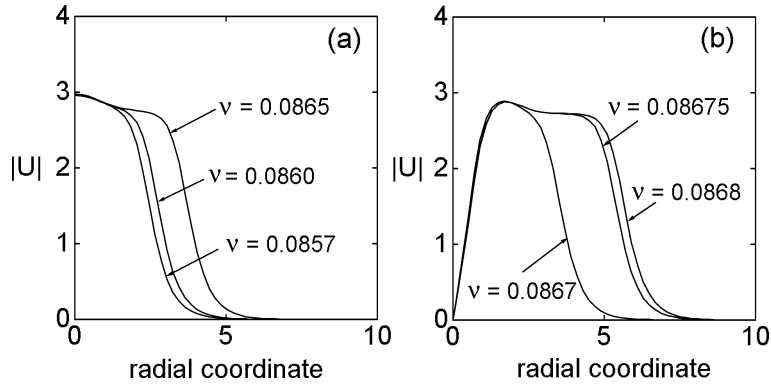


Fig. 5. Radial profiles of (a) nonspirling,  $S = 0$ , and (b) spiraling,  $S = 1$ , composite solitons at slightly different values of the quintic self-focusing parameter  $\nu$ , while the other parameters are fixed:  $\beta = 0.08$ ,  $\delta = 0.1$ ,  $\mu = 0.1$  and  $\varepsilon = 0.75$ .

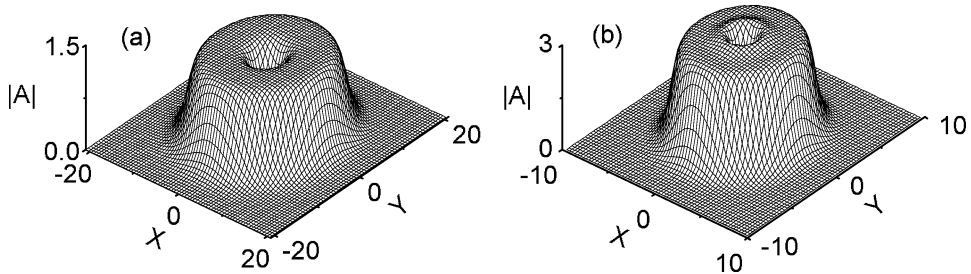


Fig. 6. Surface plots of the field of the spiraling ( $S = 1$ ) flat-top (a) and composite (b) solitons corresponding to one of the radial profiles displayed, respectively, in (a) Fig. 4 for  $\nu = 0.55$  and (b) Fig. 5 for  $\nu = 0.0868$ .

while all the composite spiraling solitons turn out to be *unstable* in direct simulations.

Calculations of the instability growth rates within the framework of Eq. (2) linearized around the composite solitons with  $S = 1$  yield results which comply with direct simulation of the nonlinear propagation in Eq. (1) written in the Cartesian coordinates. The outcome is that all the spiral composite solitons are unstable against perturbations breaking their axial symmetry. Moreover, wider composite solitons, which resemble their flat-top counterparts, are less unstable (their instability growth rate is smaller) than narrower ones. For example, the real parts of the complex instability growth rate for the spiral composite solitons presented in Fig. 5(b), which correspond to the perturbation azimuthal index  $n = 2$  are 0.0436, 0.0418 and 0.0396 for  $\nu = 0.0867$ , 0.08675 and 0.0868, respectively, whereas the growth rates for the perturbation with the index  $n = 3$  are 0.08267, 0.0789 and 0.0744, for the same three different values of  $\nu$ .

Transition from the ordinary stationary pulses to the flat-top or composite ones is continuous, as is illustrated by Fig. 7. The figure shows the soliton's intensity  $I$ , which was defined in Eqs. (4), versus the quintic self-defocusing coefficient  $\nu$ . Remarkably, the dependences are very different in the cases of the flat-top and composite solitons, and the intensity takes very different values for the nonspirling and spiraling solitons, i.e., the ones with  $S = 0$  and  $S = 1$ , respectively, which is similar to the known feature of 2D solitons in conservative models of the NLS type [29–32]. In the models of that type, the intensity of the spinning soliton is always several times larger than that of the nonspinning one, which complies with the same property of the (stable) flat-top solitons in the present model, as is seen in Fig. 7(a). However, in the case of the (unstable) composite soliton, the intensity of the nonspirling soliton may *exceed* that of its spiraling counterpart, see Fig. 7(b). This very unusual feature is another drastic difference between two superficially similar types

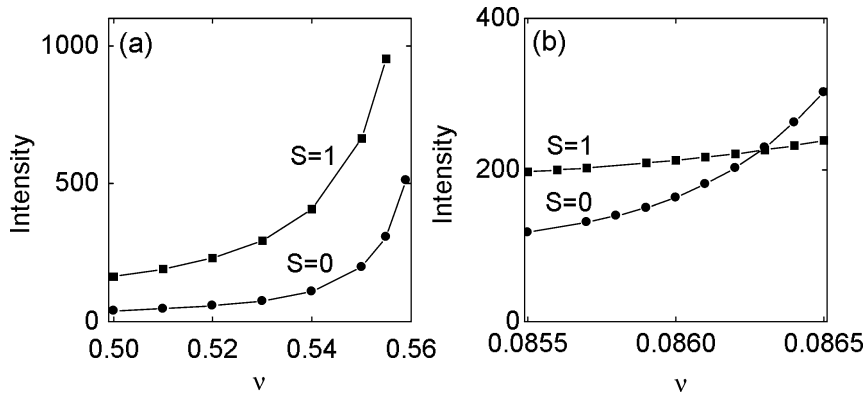


Fig. 7. Intensity of the spiraling and nonspiraling solitons vs. the quintic self-focusing coefficient  $\nu$  in the transient layer between the ordinary pulses and fronts. (a) The case of the flat-top solitons. Here,  $\beta = 0.03$ ,  $\delta = 0.05$ ,  $\mu = 0.2$  and  $\varepsilon = 0.3$ . (b) The case of the composite solitons. Here,  $\beta = 0.08$ ,  $\delta = 0.1$ ,  $\mu = 0.1$  and  $\varepsilon = 0.75$ .

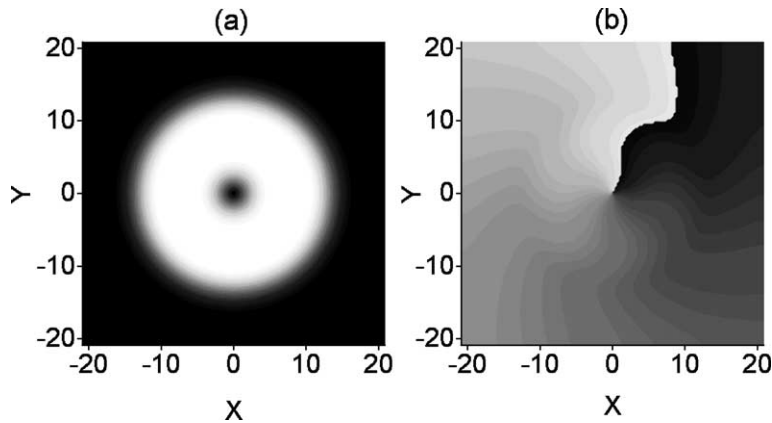


Fig. 8. Gray-scale plots of the flat-top spiral soliton created by a Gaussian beam with the intrinsic vorticity  $S = 1$ . The parameters are the same as in Fig. 6(a). (a) The absolute value  $|A|$  and (b) the phase at  $z = 200$ .

(flat-top and composite) of the broad solitons in the 2D model.

The divergence of the soliton's intensity with the increase of  $\nu$ , evident in Fig. 7, corresponds the aforementioned transition from the localized stationary axisymmetric pulses to expanding fronts. The transition takes place via the flat-top (Fig. 7(a)) or composite (Fig. 7(b)) solitons, depending on values of the system's parameters. Note that similarly looking composite solitons are known in the 1D GL model [19,20]; however, in contrast with the present 2D model, they were stable and constituted a distinct family of solitons, apart from the ordinary stationary pulses. Thus,

in the 1D model the composite solitons *did not* play the role of a transient between the ordinary pulses and fronts.

Our extensive numerical simulations of the stability have shown that the flat-top spiraling solitons are stable, in contrast to the composite ones, see above. Moreover, similar to the ordinary stable 2D spiral solitons studied in Ref. [24], the flat-top ones behave as strong *attractors*. This is proved by numerical experiments in which Gaussian pulses that were lent the intrinsic vorticity  $S = 1$ , but had shapes very different from those of the stationary flat-top solitons with the same vorticity, are launched. In spite of the great

shape difference, the initial Gaussian pulses quickly rearrange themselves and readily self-trap into the flat-top solitons. For illustration, in Fig. 8 we display gray-scale plots of the amplitude and phase of the flat-top soliton created this way from a Gaussian pulse with a nested vortex. It proves to be exactly the same stationary pulse as the one whose three-dimensional image is shown in Fig. 6(a).

#### 4. Conclusion

We have revisited the recently introduced two-dimensional isotropic Ginzburg–Landau model of the cubic–quintic type, in order to find new classes of spiraling and nonspiraling axisymmetric localized patterns in it. The first newly found species are nonstationary “erupting” solitons whose distinctive feature are irregularly repeating limited bursts. Nonspiraling (zero-spin) and spiraling (with the spin  $S = 1$ ) solitons of this type may coexist with each other, but they do not coexist with the ordinary stationary stable solitons having the same spin. The spiraling erupting solitons are shown to be unstable against azimuthal perturbations. Additionally, we have found that the recently discovered transition from ordinary stationary pulses to expanding circular fronts does not take place by a jump, but, instead, it goes via very broad stationary solitons (both nonspiraling and spiraling), which may be of two different types, depending on values of the system’s parameters: “flat-top” solitons, which are stable, or unstable “composite” solitons, that, unlike the “flat-top” ones, have some weakly pronounced intrinsic structure.

The most straightforward physical realization of the model may be provided by spatial light beam propagation in a bulk nonlinear optical material featuring losses and nonlinear gain. In particular, irregular bursts characteristic to the erupting solitons can be observed, at the output face of the sample, in the form of irregular oscillations of the beam’s power with the variation of the intensity of a pump signal providing for the (nonlinear) intrinsic optical gain in the material.

#### References

- [1] M.C. Cross, P.C. Hohenberg, *Rev. Mod. Phys.* 65 (1993) 851.
- [2] A.M. Sergeev, V.I. Petviashvili, *Dokl. AN SSSR* 276 (1984) 1380, *Sov. Phys. Dokl.* 29 (1984) 493.
- [3] B.A. Malomed, *Physica D* 29 (1987) 155, see Appendix.
- [4] O. Thual, S. Fauve, *J. Phys. (Paris)* 49 (1988) 1829.
- [5] W. van Saarloos, P. Hohenberg, *Phys. Rev. Lett.* 64 (1990) 749.
- [6] V. Hakim, P. Jakobsen, Y. Pomeau, *Europhys. Lett.* 11 (1990) 19.
- [7] B.A. Malomed, A.A. Nepomnyashchy, *Phys. Rev. A* 42 (1990) 6009.
- [8] B.A. Malomed, H.G. Winful, *Phys. Rev. E* 53 (1996) 5365.
- [9] J. Atai, B.A. Malomed, *Phys. Rev. E* 54 (1996) 4371.
- [10] J. Atai, B.A. Malomed, *Phys. Lett. A* 246 (1998) 412.
- [11] H.R. Brand, R.J. Deissler, *Phys. Rev. Lett.* 63 (1989) 2801.
- [12] R.J. Deissler, H.R. Brand, *Phys. Rev. Lett.* 72 (1994) 478.
- [13] R.J. Deissler, H.R. Brand, *Phys. Rev. Lett.* 74 (1995) 4847.
- [14] R.J. Deissler, H.R. Brand, *Phys. Rev. Lett.* 81 (1998) 3856.
- [15] H. Sakaguchi, B.A. Malomed, *Physica D* 147 (2000) 273.
- [16] V.V. Afanasjev, N. Akhmediev, J.M. Soto-Crespo, *Phys. Rev. E* 53 (1996) 1931.
- [17] N. Akhmediev, V.V. Afanasjev, *Phys. Rev. Lett.* 75 (1995) 2320.
- [18] N.N. Akhmediev, V.V. Afanasjev, J.M. Soto-Crespo, *Phys. Rev. E* 53 (1996) 1190.
- [19] J.M. Soto-Crespo, N. Akhmediev, A. Ankiewicz, *Phys. Rev. Lett.* 85 (2000) 2937.
- [20] N. Akhmediev, J.M. Soto-Crespo, G. Town, *Phys. Rev. E* 63 (2001) 056602.
- [21] B.S. Kerner, V.V. Osipov, *Autosolitons*, Kluwer Academic, Dordrecht, 1994.
- [22] N. Akhmediev, A.S. Rodrigues, G.E. Town, *Opt. Commun.* 187 (2000) 419.
- [23] L.-C. Crasovan, B. Malomed, D. Mihalache, F. Lederer, *Phys. Rev. E* 59 (1999) 7173.
- [24] L.-C. Crasovan, B.A. Malomed, D. Mihalache, *Phys. Rev. E* 63 (2001) 016605.
- [25] P. Couillet, L. Gil, D. Repaux, *Phys. Rev. Lett.* 62 (1989) 2957.
- [26] L.M. Pismen, *Vortices in Nonlinear Fields*, Oxford University Press, Oxford, 1999.
- [27] I. Aranson, V. Steinberg, *Phys. Rev. B* 53 (1996) 75.
- [28] I.S. Aranson, L.M. Pismen, *Phys. Rev. Lett.* 84 (2000) 634.
- [29] D. Mihalache, D. Mazilu, L.-C. Crasovan, B.A. Malomed, F. Lederer, *Phys. Rev. E* 61 (2000) 7142.
- [30] D.V. Petrov, L. Torner, J. Martorell, R. Vilaseca, J.P. Torres, C. Cojocaru, *Opt. Lett.* 23 (1998) 1444.
- [31] M. Quiroga-Teixeiro, H. Michinel, *J. Opt. Soc. Am. B* 14 (1997) 2004.
- [32] A. Desyatnikov, A. Maimistov, B.A. Malomed, *Phys. Rev. E* 61 (2000) 3107.